The Astrophysical Journal, 699:2017–2025, 2009 July 10 doi:10.1088/0004-637X/699/2/2017

THE RISE OF THE AGB IN THE GALACTIC HALO: Mg ISOTOPIC RATIOS AND HIGH PRECISION ELEMENTAL ABUNDANCES IN M71 GIANTS*

J. Meléndez[1] and J. G. Cohen[2]
[1] Centro de Astrofísica da Universidade do Porto, Rua das Estrelas, 4150-762 Porto, Portugal; jorge@astro.up.pt
[2] Palomar Observatory, Mail Stop 105-24, California Institute of Technology, Pasadena, California 91125, USA; jlc@astro.caltech.edu
Received 2009 January 8; accepted 2009 May 14; published 2009 June 26

ABSTRACT

High-resolution ($R \approx 100{,}000$), high signal-to-noise spectra of M71 giants have been obtained with High Resolution Echelle Spectrometer at the Keck I telescope in order to measure their Mg isotopic ratios, as well as elemental abundances of C, N, O, Na, Mg, Al, Si, Ca, Ti, Ni, Zr, and La. We demonstrate that M71 has two populations, the first having weak CN, normal O, Na, Mg, and Al, and a low ratio of ^{26}Mg/Mg (∼4%) consistent with models of galactic chemical evolution with no contribution from asymptotic giant branch (AGB) stars. The Galactic halo could have been formed from the dissolution of globular clusters prior to their intermediate-mass stars reaching the AGB. The second population has enhanced Na and Al accompanied by lower O and by higher ^{26}Mg/Mg (∼8%), consistent with models which do incorporate ejecta from AGB stars via normal stellar winds. All the M71 giants have identical [Fe/H], [Si/Fe], [Ca/Fe], [Ti/Fe], and [Ni/Fe] to within $\sigma = 0.04$ dex (10%). We therefore infer that the timescale for formation of the first generation of stars we see today in this globular cluster must be sufficiently short to avoid a contribution from AGB stars, i.e., less than ∼0.3 Gyr. Furthermore, the Mg isotopic ratios in the second M71 population, combined with their elemental abundances for the light elements, demonstrate that the difference must be the result of adding in the ejecta of intermediate-mass AGB stars. Finally, we suggest that the low amplitude of the abundance variations of the light elements within M71 is due to a combination of its low mass and its relatively high Fe-metallicity.

Key words: globular clusters: individual (M71) – stars: abundances – stars: atmospheres – stars: evolution

1. INTRODUCTION

Galactic globular clusters (GCs) show star-to-star variations in the light elements including Li, C, N, O, Na, Mg, and Al discovered more than 30 years ago. Correlations and anticorrelations among O, Na, Mg, and Al are seen in essentially all GCs, but not in field stars, as reviewed by Gratton et al. (2004). These correlations are highly suggestive of proton burning of H at high temperatures (Denisenkov & Denisenkova 1990). However, detection of these correlations among GC main-sequence stars which have not yet evolved sufficiently for their central temperatures to become hot enough for the necessary nuclear reactions to operate by Gratton et al. (2001) and by Ramírez & Cohen (2002) demonstrated definitively that these patterns are imprinted from an external source; they cannot be the result of internal nucleosynthesis followed by mixing to the surface of processed material. Cohen et al. (2005) have shown that superposed on this is the imprint of mixing of material processed through H-burning via the CN cycle, but only among the most luminous of the globular cluster giants.

The scenario generally invoked to explain this is that more than one generation of stars was formed in the GC; first one that produced the heavy elements we see today within a system where the gas was well mixed throughout the entire volume. This was followed by the second generation of stars, including low mass stars that survive to the present, then a subsequent stellar generation formed from gas contaminated by the ejecta of an earlier generation that was not uniformly mixed throughout the volume. It is generally presumed that material processed within the interiors of asymptotic giant branch (AGB) stars, mixed to the stellar surface, then ejected by stellar winds, is the culprit producing the star-to-star variations detected among GC stars (see e.g., Fenner et al. 2003; Cohen et al. 2005; Ventura & D'Antona 2008, and references therein). Recently, rapidly rotating massive stars have also been invoked for this purpose as during their main-sequence phase they transport material processed through H-burning at high temperatures to their surfaces, see e.g., Decressin et al. (2007). This material has an escape velocity low enough to be confined to the cluster, unlike that of the subsequent radiatively driven winds or the eventual SN, where the ejected material has such a high velocity that it is lost by the cluster.

However, some of the details of the behavior seen thus far do not match the predictions for high temperature H-burning. The most discrepant case is that of the Mg isotopes. The first attempt to measure Mg isotopic ratios for GC giants was by Shetrone (1996), with additional recent studies by Yong et al. (2003, 2006). All of these authors found substantial contributions from the heavier Mg isotopes, reaching up to half of the total Mg, far larger than the solar ratio, which is 79:10:11 for ^{24}Mg:^{25}Mg:^{26}Mg. Measurement of the Mg isotopic ratios requires detection of weak contributions from the rarer heavier Mg isotopes in the wings of much stronger ^{24}MgH lines, hence exquisite spectra of very high spectral resolution (∼100,000) and very high signal-to-noise ratio (S/N), as well as careful attention to details of the line list used for the spectral synthesis and to the analysis procedure.

Here we present a new attempt to measure the Mg isotopic ratios in the giants of the relatively metal-rich GC M71 which we hope fulfills the criteria described above to achieve a reliable result. We exploit our exquisite spectra to derive precision abundances for several additional elements in M71, including the light elements O, Mg, Na, and Al. We discuss our results in

* Based on observations obtained at the W.M. Keck Observatory, which is operated jointly by the California Institute of Technology, the University of California and the National Aeronautics and Space Administration.

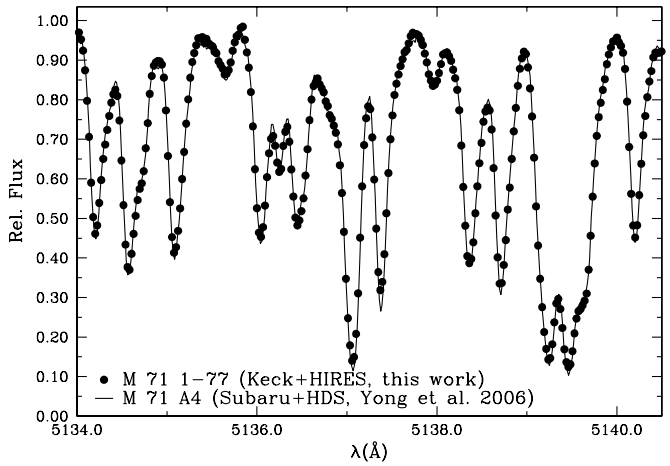

Figure 1. Comparison of M71 1−77 (Keck I + HIRES, this work) and M71 A4 (Subaru + HDS; Yong et al. 2006). Both stars have similar stellar parameters ($T_{\rm eff} \approx 3900$ K), except that A4 has a lower macroturbulence. Both spectra were taken with a resolving power of $\approx 10^5$.

the context of the history of star formation in globular clusters, and the contribution of AGB stars to GCs and to the halo field.

2. OBSERVATIONS

The sample consists of nine giant stars in the globular cluster M71, eight observed with HIRES (Vogt et al. 1994) at the Keck I telescope by us and one (M71 A4) observed with the High Dispersion Spectrograph (HDS) at the Subaru telescope by Yong et al. (2006).[3]

The Keck observations were obtained in 2004 August, 2005 June, and 2007 September. All our data were obtained after the HIRES upgrade (2004 August), thus taking advantage of improvements in efficiency, spectral coverage, and spectral resolution. A resolving power of $R \approx 10^5$ was achieved using a 0.″4 wide slit, accepting a substantial light loss at the slit in order to achieve the necessary spectral resolution. The signal-to-noise level exceeded 100 pixel^{-1}, with 1.3 km s^{-1} pixel^{-1}. In Figure 1, we compare our HIRES spectrum of M71 1−77 with the HDS spectrum of M71 A4 (Yong et al. 2006), which is of similar quality ($R \approx 90{,}000$).

The spectral orders were extracted using both IRAF and MAKEE.[4] Further data reductions (Doppler correction, continuum normalization, and combining spectra) were performed with IRAF.

3. ANALYSIS

Initially stellar parameters were obtained from photometry, following the precepts set out in Cohen et al. (2001). We are fortunate to now have J and K_s photometry from Two micron All Sky Survey (2MASS; Skrutskie et al. 1997; Cutri et al. 2003; not available at the time of the initial M71 abundance study) and optical photometry with more extensive coverage of the area of M71 from Stetson (2000) as updated on his on-line database available through the CADC. We adopt E($B-V$) = 0.25 mag from the 2003 February version of the online database of Harris (1996).[5]

Our preliminary analysis using the photometric stellar parameters and Kurucz overshooting model atmospheres (Castelli et al. 1997) revealed that M71 seems to show only very slight abundance variations (if any) in some elements (e.g., Mg), and therefore very high precision is needed to ascertain if abundance variations are present or not. Seeking the highest possible precision, and given the potential presence of reddening variations across the field of M71, we decided to perform the analysis using spectroscopically determined stellar parameters. The stars have similar temperatures ($T_{\rm eff} = 4045 \pm 225$ K), so this approach should minimize errors in the *relative* stellar parameters.

Excitation and ionization balances of Fe I and Fe II were performed with the 2002 version of MOOG (Sneden 1973), using the Fe I line list of Alves-Brito et al. (2009, in preparation) and the Fe II line list of Hekker & Melendez (2007), which is described in Meléndez & Barbuy (2009). These line lists have been carefully scrutinized to avoid significant blends (e.g., CN) in metal-rich cool giants. All equivalent widths were measured by hand using IRAF, employing the deblend option when necessary. Microturbulence was obtained by flattening the trend in the iron abundance from Fe I lines versus reduced equivalent width. The zero points of our spectroscopic stellar parameters have been determined by Meléndez et al. (2008) using many bright field giants with precise effective temperatures using the infrared flux method temperature scale of Ramírez & Meléndez (2005), and with surface gravities determined with *Hipparcos* parallaxes and Yonsei-Yale (Demarque et al. 2004) and Padova isochrones (da Silva et al. 2006).

Once the stellar parameters ($T_{\rm eff}$, log g, $v_{\rm mic}$) were set, the macroturbulence ($v_{\rm mac}$) was determined employing five Fe I lines (605.60, 607.85, 609.67, 612.02, 615.16 nm) and checked with other lines present in the same region (605 to 615 nm). Note that in previous works on Mg isotopic ratios (e.g., McWilliam & Lambert 1988; Yong et al. 2003) only the Ni I 511.54 nm and the Ti I 514.55 nm were used to obtain the macroturbulent broadening. However, we find that these lines are not useful in metal-rich cool giants, because the region around each of them is badly blended. The region we have chosen to use for this purpose (605–615 nm) is much cleaner, although we have also included in our spectrum synthesis blends by atomic, C_2, and CN lines. We recommend the use of this region to determine $v_{\rm mac}$ in future studies of Mg isotopic ratios in relatively metal-rich very cool stars.

The line lists of MgH and C_2 (0-0 band) have been previously described in Meléndez & Cohen (2007), and the extension of our C_2 line list to other bands is described in Meléndez & Asplund (2008). The CN line list adopted here is from Meléndez & Barbuy (1999). For the atomic lines, we have used when available transition probabilities based on laboratory measurements, otherwise we have adopted astrophysical gf-values based on Arcturus. We only used the best, most isolated atomic lines within the wavelength range covered by our spectra, listed in Table 1.

The Mg isotopic ratios were determined by spectral synthesis, as described in Meléndez & Cohen (2007), except that in cool metal-rich giants the MgH feature at 513.46 nm (usually employed for Mg isotopic ratios; e.g., Gay & Lambert 2000) seems blended, so instead we use the 513.43 nm feature. Two other MgH features at 513.87 and 514.02 nm (e.g., Yong et al. 2003; Meléndez & Cohen 2007) were also used for obtaining the Mg isotopic ratios. After the first trials, it was clear that the ^{24}Mg:^{25}Mg:^{26}Mg ratios were no larger than terrestrial (79:10:11), therefore we have computed synthetic spectra with

[3] The spectrum of M71 A4 has been kindly made available to us by D. Yong and W. Aoki.

[4] MAKEE was developed by T. A. Barlow specifically for reduction of Keck HIRES data. It is freely available at http://www2.keck.hawaii.edu/realpublic/inst/hires/data_reduction.html.

[5] http://physwww.mcmaster.ca/~harris/Databases.html.

Table 1
List of Atomic Lines Used

Wavelength (Å)	Exc. Pot. (eV)	log(*gf*) (dex)	Species
6300.30	0.000	−9.72	[O I]
6363.77	0.020	−10.19	[O I]
6154.22	2.102	−1.547	Na I
6160.74	2.104	−1.246	Na I
6318.71	5.108	−1.945	Mg I
6319.23	5.108	−2.165	Mg I
6696.01	3.143	−1.481	Al I
6698.66	3.143	−1.782	Al I
5488.98	5.614	−1.69	Si I
6142.48	5.619	−1.41	Si I
5590.11	2.521	−0.571	Ca I
5867.56	2.933	−1.57	Ca I
6156.02	2.521	−2.42	Ca I
6166.43	2.521	−1.142	Ca I
5453.64	1.443	−1.61	Ti I
5648.56	2.495	−0.25	Ti I
5913.71	0.021	−4.10	Ti I
5918.53	1.066	−1.47	Ti I
6092.79	1.887	−1.378	Ti I
6273.38	0.021	−4.17	Ti I
6706.29	1.502	−2.78	Ti I
5435.85	1.986	−2.60	Ni I
5468.10	3.847	−1.61	Ni I
5589.35	3.898	−1.14	Ni I
5846.99	1.676	−3.21	Ni I
6086.28	4.266	−0.51	Ni I
6108.11	1.676	−2.44	Ni I
6130.13	4.266	−0.96	Ni I
6127.45	0.154	−1.06	Zr I
6134.55	0.000	−1.28	Zr I
6140.53	0.519	−1.41	Zr I
6143.20	0.071	−1.10	Zr I
6390.48	0.321	−1.41	La II

isotopic ratios ranging from ^{24}Mg:^{25}Mg:^{26}Mg = 100:0:0 to 76:12:12.

The isotopic ratios were determined by χ^2 fits, by computing $\chi^2 = \Sigma(O_i - S_i)/\sigma^2$, where O_i and S_i represents the observed and synthetic spectrum, respectively, and $\sigma = (S/N)^{-1}$. Examples of the χ^2 fits are shown in Figures 2 and 3 for the three recommended MgH features. The resulting Mg isotope ratios are presented in Table 2. In this table are also given the standard deviation from the three different MgH features, which for ^{25}Mg and ^{26}Mg have typical values of σ = 1.7% and 1.9%, respectively, corresponding to standard errors of 1.0% and 1.1%. As discussed below, the true error for ^{26}Mg is actually somewhat smaller than for ^{25}Mg. Due to the larger isotopic separation of the ^{26}MgH lines, the determination of ^{26}Mg/^{24}Mg is more reliable than ^{25}Mg/^{24}Mg.

The elemental abundances of C, N, O, Na, Mg, and Al were obtained by spectral synthesis, taking into account blends by atomic, C_2 and CN lines, and the abundances of Si, Ca, Ti, Ni and Zr were obtained from equivalent widths. Carbon abundances were obtained from C_2 lines around 563 nm and checked using CH lines around 430 nm (Plez et al. 2008, see also Plez & Cohen 2005). Nitrogen abundances were obtained using CN lines around 630–637 nm and 669–671 nm. The CN-rich stars have N abundances ∼3 times higher than the CN-weak stars, but the difference may be higher because TiO blends prevent a precise determination of N abundances in the CN-weak stars. The elemental abundance ratios are given in Tables 2 and 3.

The iron abundances, [C,N,O/Fe] abundance ratios, and the C+N and C+N+O abundance sums, are shown in Figure 4 as a function of effective temperature. A similar plot for the isotopic ^{24,25,26}Mg/Mg, ^{25,26}Mg/^{24}Mg ratios and the elemental abundance ratios [Na,Mg,Al/Fe] is presented in Figure 5, and the [Si,Ca,Ti,Ni,Zr,La/Fe] ratios are shown in Figure 6.

In these and subsequent figures, CN-weak and CN-rich giants are represented by the open and filled circles, respectively. The CN status of our sample stars have been obtained from Smith & Norris (1982) and Lee (2005), except for star M71 I, for which no previous information on its CN bands is available in the literature. Since this star shows strong CN bands in our HIRES spectrum, we have also included it as a CN-strong star.

As discussed below, some abundance ratios show trends with $T_{\rm eff}$. The coefficients of the fits for the CN-weak stars are given in Table 4.

4. DISCUSSION

4.1. Correlations between ^{24,25,26}Mg/Mg, O, Na, Mg, and Al

The Mg isotopic ratios and the elemental abundances of O, Na, Mg, and Al for the CN-weak stars seem to show some trend with effective temperature, probably due to NLTE and three-dimensional effects (Asplund 2005; Collet et al. 2007). After correcting for trends with $T_{\rm eff}$, the scatter in [O,Na,Mg,Al/Fe] for the CN-weak stars is only 0.018, 0.039, 0.018 and 0.021 dex, respectively. The CN-rich stars depart from the behavior of the CN-weak stars, showing larger ^{25,26}Mg/Mg ratios, larger Na and Al elemental abundances, and lower O and Mg elemental abundances.

In Figures 7–11 are shown the ^{24}Mg/Mg, ^{25}Mg/Mg, ^{25}Mg/^{24}Mg, ^{26}Mg/Mg, and ^{26}Mg/^{24}Mg ratios as a function of [O,Na,Mg,Al/Fe]. In these plots the trend with effective temperature (Figures 4 and 5, Table 4) has been corrected in the [O,Na,Mg,Al/Fe] ratios, to prevent spurious trends. The ^{25,26}Mg/^{24}Mg isotopic ratios show a larger spread than ^{25,26}Mg/Mg due to the spread in ^{24}Mg/Mg (CN-rich giants show lower ^{24}Mg/Mg than CN-weak giants).

In Figure 7, we show that ^{24}Mg in CN-rich stars is anticorrelated with Na and probably also with Al. The ^{25}Mg/Mg ratios are less reliable than the ^{26}Mg/Mg ratios. Although Table 2 suggests higher uncertainties for ^{26}Mg than for ^{25}Mg, with standard errors of 1.1% and 1.0%, respectively, the star-to-star scatter for the CN-weak stars actually shows that the errors for ^{25}Mg and ^{26}Mg are 0.9% and 0.8%, respectively, i.e., in both cases somewhat lower than the errors estimated from Table 2. The higher error bar (±0.9%) for ^{25}Mg is expected due to the smaller isotopic shift of the ^{25}MgH lines. Hence, ^{25}Mg does not show clear trends besides the fact that ^{25}Mg is enhanced in CN-rich giants (Figures 8 and 9). The CN-weak stars do not show any correlation between ^{26}Mg and the elemental abundances of Na, O, Mg, and Al (Figures 10 and 11), but the CN-rich giants show strong, weak, and no correlations between ^{26}Mg and the elemental abundances of Na and Al, O, and Mg, respectively.

Figure 12 shows the correlations between the elemental abundances of O, Na, Mg, and Al, which have been corrected for trends with $T_{\rm eff}$ (Figures 4 and 5, Table 4), and therefore any remaining trend or scatter should be real. Interestingly, even though the CN-weak stars show only small scatter in their abundances ratios (0.02–0.04 dex), and seem to be roughly constant between the uncertainties, there is a hint of a correlation between Na and Al. On the other hand, Al and Mg, and O and

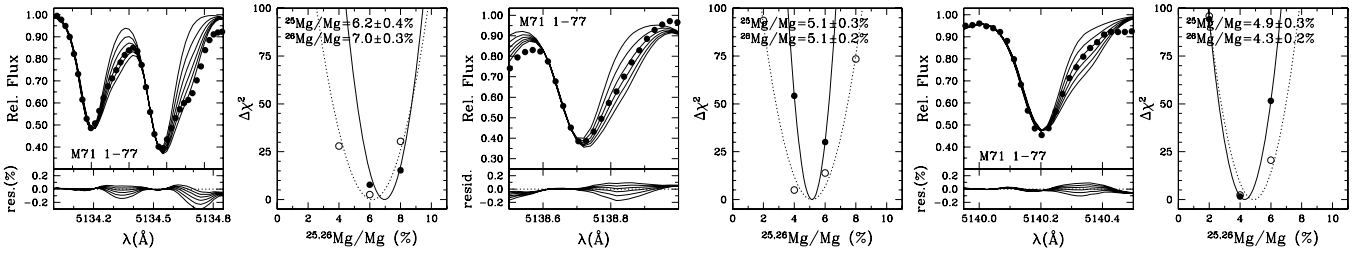

Figure 2. Fits for the 5134.3 Å (left), 5138.7 Å (center), and 5140.2 Å (right) MgH features in the giant M71 1−77. Observed spectra are represented as filled circles, and synthetic spectra as solid lines. The calculations were performed for ^{25,26}Mg/Mg ratios of 0%–10%. The relative variations of the χ^2 fits are shown as a function of the isotopic ratio.

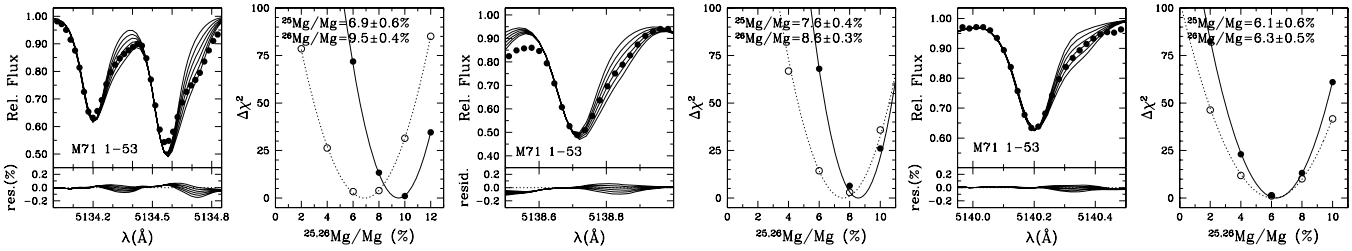

Figure 3. Fits for the 5134.3 Å (left), 5138.7 Å (center), and 5140.2 Å (right) MgH features in the giant M71 1–53. Observed spectra are represented as filled circles, and synthetic spectra as solid lines. The calculations are shown for ^{25,26}Mg/Mg ratios of 2%–12% (left panel) and 0%–10% (center and right panels). The relative variations of the χ^2 fits are shown as a function of the isotopic ratio.

Table 2
Stellar Parameters, Mg Isotopic Ratios, C, N, O, C+N, and C+N+O Abundances

Star	$T_{\rm eff}$,log g,[Fe/H],$v_{\rm mic}$,$v_{\rm mac}$,^{25}Mg/Mg,^{26}Mg/Mg	[C/Fe]	[N/Fe]	[O/Fe]	A(C)	A(N)	A(O)	A(CN)	A(CNO)
	(K, dex, dex, km s^{-1}, km s^{-1}, %, %)	(dex)	(dex)	(dex)	(dex)	(dex)	(dex)	(dex)	(dex)
1–45	3870, 0.60, −0.83, 1.65, 6.0, 8.4(1.5), 9.2(2.3)	0.16	0.75	0.32	7.76	7.75	8.26	8.06	8.47
I	4080, 1.20, −0.78, 1.52, 5.2, 6.8(1.7), 6.9(1.9)	0.13	0.60	0.49	7.78	7.65	8.48	8.02	8.61
1–66	4150, 1.50, −0.79, 1.49, 5.6, 6.9(1.9), 7.7(2.5)	0.12	0.86	0.45	7.76	7.90	8.43	8.14	8.61
1–53	4150, 1.50, −0.78, 1.52, 5.6, 6.9(0.8), 8.1(1.6)	0.01	0.91	0.40	7.66	7.96	8.39	8.14	8.58
1–46	3820, 0.45, −0.81, 1.65, 6.0, 5.9(1.7), 6.0(2.2)	0.18	−0.03	0.39	7.81	7.00	8.36	7.87	8.48
A4	3870, 0.50, −0.81, 1.52, 5.5, 3.9(1.7), 5.0(2.1)	0.17	0.28	0.42	7.79	7.30	8.38	7.91	8.51
1–77	3900, 0.55, −0.80, 1.57, 5.9, 5.2(1.0), 5.7(1.2)	0.17	0.22	0.40	7.80	7.25	8.37	7.91	8.50
1–64	4160, 1.40, −0.76, 1.54, 5.2, 5.9(2.1), 6.0(1.8)	0.05	0.38	0.49	7.72	7.45	8.50	7.91	8.60
1–21	4270, 1.45, −0.84, 1.65, 6.0, 5.2(1.9), 3.9(1.6)	0.19	0.39	0.58	7.78	7.38	8.51	7.93	8.61

Notes. The scatter (σ) of the ^{25,26}Mg/Mg ratios obtained between the three MgH features is given between parenthesis. The first four stars are CN-strong giants and the other five stars are CN-weak giants.

Na, seem to be anticorrelated, although the evidence is weaker for the O:Na anticorrelation. The CN-strong stars show strong correlation and anticorrelation between Na and Al, and O and Na, respectively.

4.2. C+N and C+N+O in M71 Giants

As can be seen in Figure 4, the C+N abundance sum is larger in CN-rich than in CN-weak M71 giants. This is mainly due to the large N enhancement of the CN-rich giants, which have N abundances ∼0.5 dex higher than the CN-weak giants. Keck low-resolution spectra of CN-weak and CN-strong main-sequence stars in M71 show that CN-strong dwarfs are also enhanced in nitrogen when compared to CN-weak dwarfs (Briley & Cohen 2001).

The C+N+O abundance sum is constant within 0.1 dex (Figure 4), in agreement with other high resolution analysis of GC giants in the literature, which find C+N+O constant within 0.3 dex for NGC 6712 ([Fe/H] = −1.0, Yong et al. 2008), M4 ([Fe/H] = −1.1, Smith et al. 2005), and M13 ([Fe/H] = −1.5, Cohen & Meléndez 2005).

Recently, Yong et al. (2009) have found a large C+N+O spread of 0.57 dex for NGC 1851 giants ([Fe/H] = −1.2). This spread

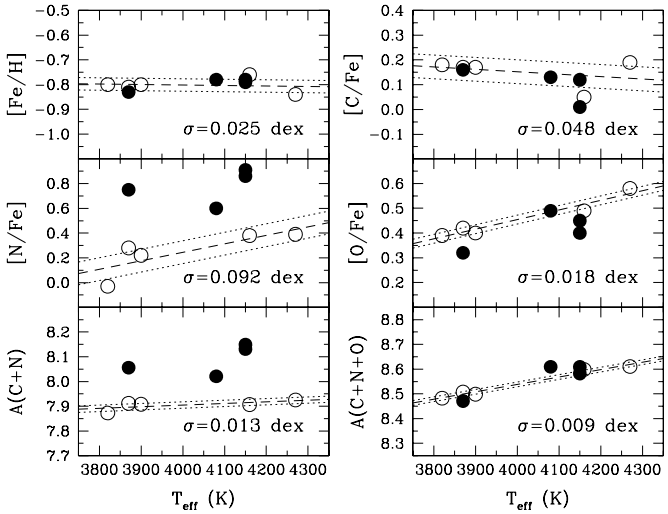

Figure 4. [Fe/H], [C,N,O/Fe], A(C+N), and A(C+N+O) abundances (dex) as a function of $T_{\rm eff}$. Open and filled circles represent CN-weak and CN-strong stars, respectively. The dashed line is a fit to the CN-weak stars, and the dotted lines show the scatter (σ) around the fit.

Table 3
[Na,Mg,Al,Si,Ca,Ti,Ni,Zr,La/Fe] Abundance Ratios

Star	[Na/Fe] (dex)	[Mg/Fe] (dex)	[Al/Fe] (dex)	[Si/Fe] (dex)	[Ca/Fe] (dex)	[Ti/Fe] (dex)	[Ni/Fe] (dex)	[Zr/Fe] (dex)	[La/Fe] (dex)
1–45	0.48	0.21	0.36	0.20	0.18	0.29	−0.02	0.23	0.37
I	−0.03	0.15	0.20	0.19	0.16	0.18	−0.04	0.06	0.29
1–66	0.17	0.14	0.25	0.26	0.16	0.17	−0.01	0.08	0.36?
1–53	0.26	0.17	0.28	0.22	0.19	0.22	0.00	0.12	0.43?
1–46	0.02	0.25	0.26	0.16	0.10	0.27	−0.06	0.16	0.30
A4	0.00	0.24	0.26	0.15	0.18	0.29	−0.02	0.17	0.29
1–77	0.08	0.19	0.30	0.12	0.22	0.33	−0.02	0.23	0.28
1–64	0.01	0.18	0.23	0.18	0.20	0.22	−0.04	0.12	0.29
1–21	−0.09	0.18	0.18	0.24	0.15	0.12	−0.04	−0.05	0.23

Note. The first four stars are CN-strong giants and the other five stars are CN-weak giants.

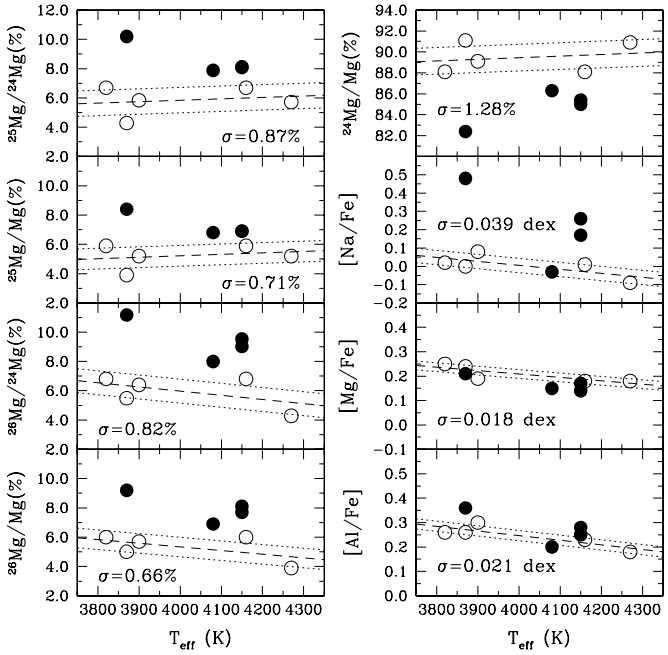

Figure 5. ^{24,25,26}Mg/Mg ratios and [Na,Mg,Al/Fe] abundance ratios (dex) as a function of $T_{\rm eff}$. Open and filled circles represent CN-weak and CN-strong stars, respectively. The dashed line is a fit to the CN-weak stars, and the dotted lines show the scatter (σ) around the fit.

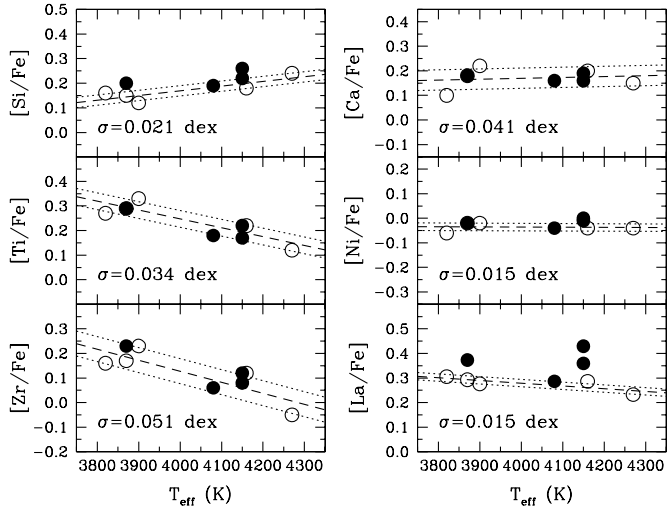

Figure 6. [Si,Ca,Ti,Ni,Zr,La/Fe] abundance ratios (dex) as a function of $T_{\rm eff}$. Open and filled circles represent CN-weak and CN-strong stars, respectively. The dashed line is a fit to the CN-weak stars, and the dotted lines show the scatter (σ) around the fit.

exceeds their estimated uncertainty (0.14 dex), and is much larger than that observed in other GCs, where no significant spread is found. Yong et al. (2009) interpret the large spread in C+N+O as a signature of AGB pollution in NGC 1851, and they conclude that if the AGB scenario is applicable to other GCs with constant C+N+O, then perhaps the masses of the AGB polluting stars in NGC 1851 were lower than in other GCs. This is probably also the reason why NGC 1851, unlike other GCs, shows a large spread in the *s*-process elements Zr and La (Yong et al. 2009).

4.3. Chemical Evolution of the Mg Isotopes

As discussed in Meléndez & Cohen (2007), the lightest and most abundant Mg isotope can be formed in massive stars (e.g., Woosley & Weaver 1995) as a primary isotope from H. The heavier isotopes are formed as secondary isotopes, as well as in intermediate-mass AGB stars (Karakas & Lattanzio 2007), so the isotopic ratios ^{25,26}Mg/^{24}Mg increase with the onset of AGB stars. Therefore, Mg isotopic ratios in halo stars can be used as a chronometer to constrain the rise of the AGB in our Galaxy. In our earlier paper, we applied this technique to a sample of metal-poor Galactic halo field dwarfs to establish that the AGB

Table 4
Abundance Trends with Temperature (A = C + slope * $T_{\rm eff}$) for the CN-weak Giants

Abundance	C (dex)	slope (dex K^{-1})
[Fe/H]	−0.7243	−1.9401E-05
[C/Fe]	0.5388	−9.6626E-05
[N/Fe]	−2.4973	6.8564E-04
[O/Fe]	−1.0946	3.8726E-04
[Na/Fe]	0.8767	−2.1798E-04
[Mg/Fe]	0.7654	−1.3923E-04
[Al/Fe]	1.0106	−1.9097E-04
[Si/Fe]	−0.5890	1.8957E-04
[Ca/Fe]	0.0252	3.6139E-05
[Ti/Fe]	1.6833	−3.5899E-04
[Ni/Fe]	−0.0085	−6.8475E-06
[Zr/Fe]	1.9213	−4.4838E-04
[La/Fe]	0.7269	−1.1193E-04
A(C+N)	7.6377	6.6801E-05
A(C+N+O)	7.3416	2.9914E-04

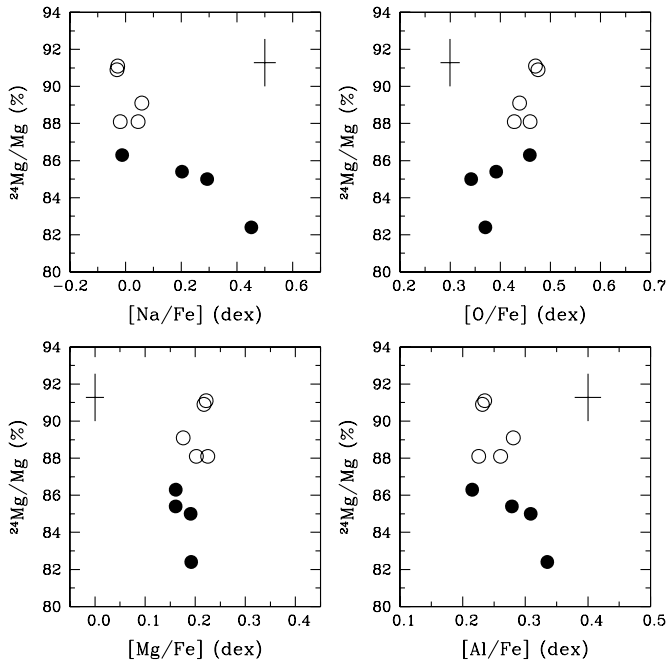

Figure 7. ^{24}Mg/Mg ratios as a function of [Na/Fe], [O/Fe], [Mg/Fe], and [Al/Fe]. Open and filled circles represent CN-weak and CN-strong stars, respectively. Trends with $T_{\rm eff}$ have been corrected for the elemental [X/Fe] ratios (O, Na, Mg, Al).

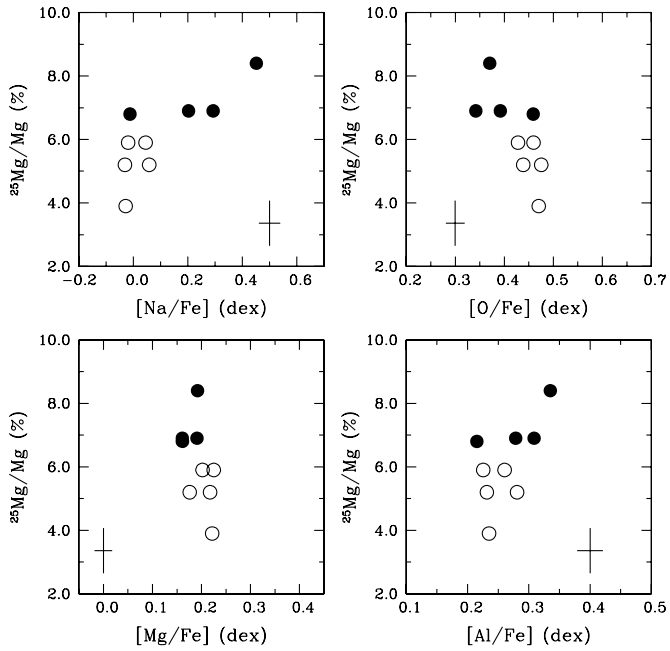

Figure 8. ^{25}Mg/Mg ratios as a function of [Na/Fe], [O/Fe], [Mg/Fe], and [Al/Fe]. Open and filled circles represent CN-weak and CN-strong stars, respectively. Trends with $T_{\rm eff}$ have been corrected for the elemental [X/Fe] ratios (O, Na, Mg, Al).

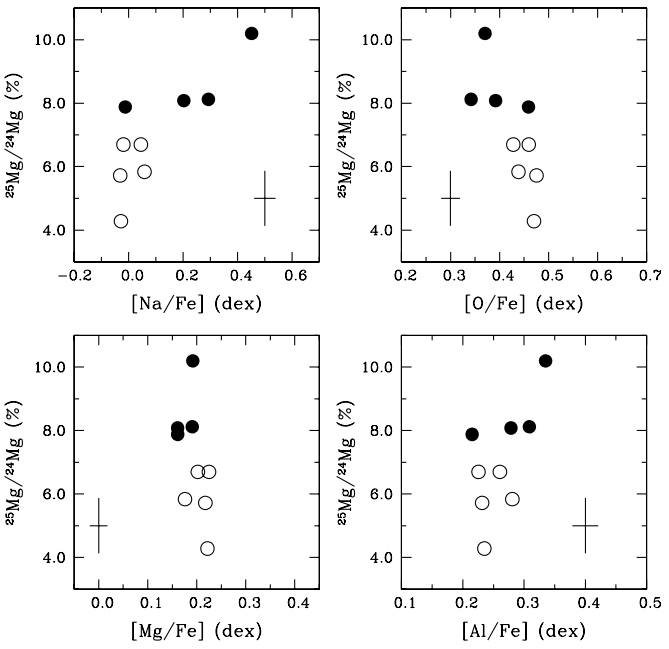

Figure 9. ^{25}Mg/^{24}Mg ratios as a function of [Na/Fe], [O/Fe], [Mg/Fe], and [Al/Fe]. Open and filled circles represent CN-weak and CN-strong stars, respectively. Trends with $T_{\rm eff}$ have been corrected for the elemental [X/Fe] ratios (O, Na, Mg, Al).

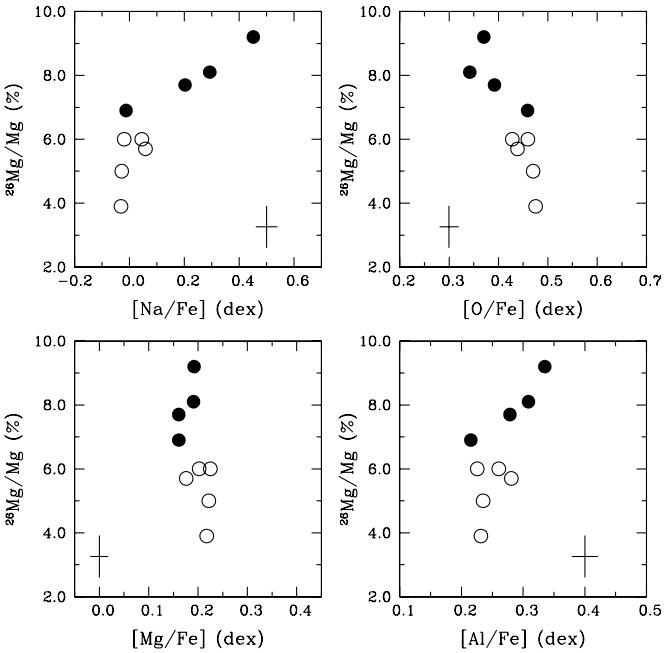

Figure 10. ^{26}Mg/Mg ratios as a function of [Na/Fe], [O/Fe], [Mg/Fe], and [Al/Fe]. Open and filled circles represent CN-weak and CN-strong stars, respectively. Trends with $T_{\rm eff}$ have been corrected for the elemental [X/Fe] ratios (O, Na, Mg, Al).

did not make a significant contribution to Mg in the Galactic halo at least until [Fe/H] ~ -1.3 dex was reached.

Figure 13 shows the chemical evolution of ^{26}Mg/^{24}Mg for halo field dwarfs (Meléndez & Cohen 2007), adding in the M71 giants, with models from Fenner et al. (2003) for the solar neighborhood both with and without the contribution of AGB stars. We see that the M71 CN-weak giants have very low Mg isotopic ratios ^{26}Mg/Mg ($\sim$4%) consistent with models of galactic chemical evolution with no contribution from AGB stars, and extending our previous results based on metal-poor halo field dwarfs to still higher metallicity. Based on the calculations of stellar yields for AGB stars by Karakas & Lattanzio (2003), updated in Karakas & Lattanzio (2007), stars of initial mass 3–6 $M_{\odot}$ are required to contribute significant amounts of the heavier Mg isotopes. Stars in this mass range reach the upper AGB at an age of $\sim$0.3 Gyr; see e.g., the

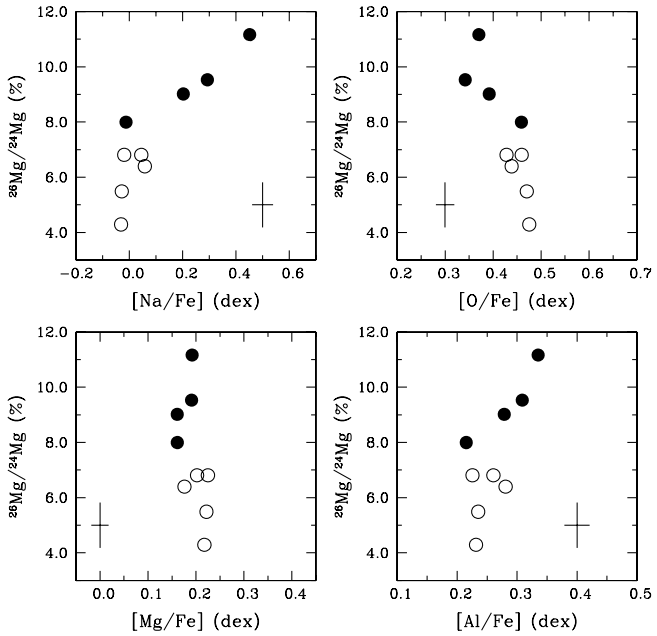

Figure 11. ^{26}Mg/^{24}Mg ratios as a function of [Na/Fe], [O/Fe], [Mg/Fe], and [Al/Fe]. Open and filled circles represent CN-weak and CN-strong stars, respectively. Trends with $T_{\rm eff}$ have been corrected for the elemental [X/Fe] ratios (O, Na, Mg, Al).

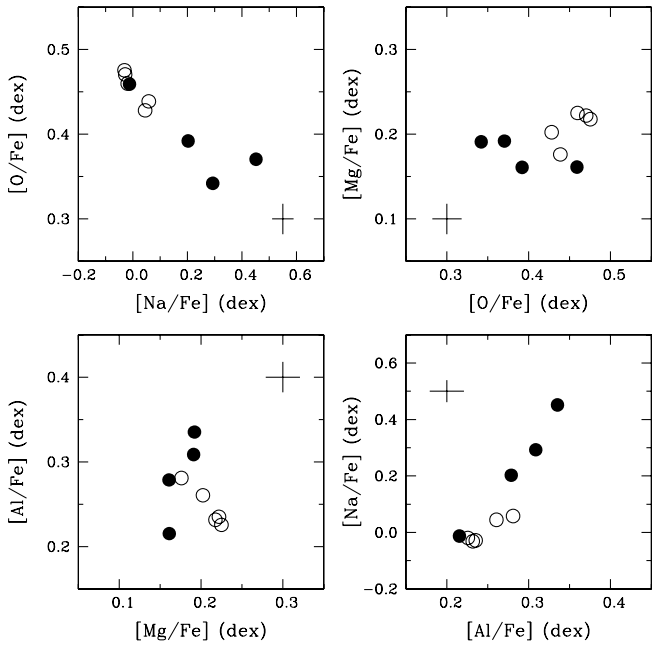

Figure 12. Correlations between O, Na, Mg, and Al. Open and filled circles represent CN-weak and CN-strong stars, respectively. The abundance ratios have been corrected for trends with $T_{\rm eff}$. A clear anticorrelation is seen between O and Na, and a well defined correlation is seen between Na and Al.

Padova evolutionary tracks.[6] For a GC as metal-rich as is M71, this timescale must reflect the minimum age difference between the CN-weak and the CN-rich stars in the GC as well as the maximum range in age of the CN-weak stars we see today in M71, assuming uniform mixing of the gas within the GC. Furthermore, the enrichment of the halo gas from which M71 eventually formed must have reached such a high Fe-metallicity without a substantial contribution from proton burning of H at high temperatures. We argue that AGB stars

[6] http://pleiadi.pd.astro.it/

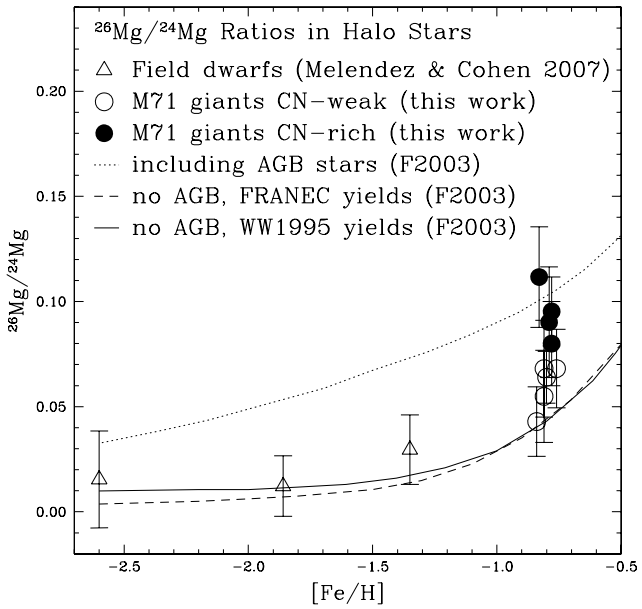

Figure 13. Our ^{26}Mg/^{24}Mg ratios in both field dwarfs (triangles; Meléndez & Cohen 2007) and M71 giants (circles; this work) as a function of [Fe/H]. Chemical evolution models by Fenner et al.(2003) including (dotted line) and excluding (solid and dashed lines) AGB stars are shown. At the metallicity of M71 ([Fe/H] = −0.8 dex) the isotopic ratios in the CN-weak stars (open circles) are explained by massive stars, but the CN-strong stars (filled circles) may have been polluted by intermediate-mass AGB stars.

are the source of the "polluted" material, rather than it coming from rapidly rotating massive stars, on the basis of timescales, which would be uncomfortably short in the latter case, and also the uniformity of the heavy elements within all stars of M71. Our precision abundances define an upper limit to the range of abundances of the heavy elements in M71; all the M71 giants have identical [Fe/H], [Si/Fe], [Ca/Fe], [Ti/Fe], and [Ni/Fe] to within $\sigma = 0.04$ dex (10%) after the trends with $T_{\rm eff}$ are removed (see Figures 4 and 6). This would be hard to achieve if massive stars were the source of polluting gas in GCs.

On the other hand, the M71 giants with strong CN (accompanied by lower O with higher Na and Al than those of the weak CN giants) show higher Mg isotopic ratios ^{26}Mg/Mg (∼8%), but these are still quite low compared to previous studies by Yong et al. (2006) mostly in GCs of lower metallicity. In particular, star M71 A4 has been also analyzed by Yong et al. (2006), who find higher isotopic ratios than ours. This must be due to the different analysis techniques, as the same observed spectrum was used. In particular, note that their macroturbulent velocity for this star is lower. As shown in Figure 13, our newly measured Mg isotope ratios for the CN-rich giants in M71 lie on the predicted curve for models which include the appropriate contribution to the chemical inventory from material processed through high-temperature H-burning which we believe comes from AGB stars during the normal course of evolution of intermediate mass stars.

4.4. Neutron Capture Processes

Figure 6 displays [La/Fe] versus $T_{\rm eff}$ for the M71 sample of luminous giants. The 6390 Å La II line was synthesized with hyperfine structure and transition probability from Lawler et al. (2001). The results are more uncertain than for most of the other elements discussed here as there is only one La II line which was sufficiently unblended to be used, and it lies within a CN band. However, there appears to be a slight excess of La among

the CN-strong M71 giants. This excess is small enough that it would not have been detected in previous analyses such as that of Ramírez & Cohen (2002), whose spectra were of lower spectral resolution and SNR, with consequent larger uncertainties.

La, together with Ba,[7] are the archetypical elements indicating a contribution to the star's chemical inventory via *s*-process neutron capture. But this provides no discrimination in the source of the *s*-process, be it intermediate mass AGB stars or young massive rotating stars. The former, especially in metal-poor AGB stars, is well known as a site for such production (Busso et al. 2001), while very recent work by the NuGrid project (Hirschi et al. 2008) demonstrates that the *s*-process can operate efficiently in rotating young massive stars.

Zr is also believed to be produced primarily in AGB stars via the *s*-process of neutron capture on Fe seeds. However, we do not see any detectable difference for the mean [Zr/Fe] between the CN-rich and the CN-weak M71 giants, while differences in the isotopic ratio ^{26}Mg/Mg are apparent, and we believe there are differences in [La/Fe] as well. There are four detected Zr I lines, so the lack of detectable star-to-star variation in [Zr/Fe] must be regarded as well established. The production of Zr in AGB stars is discussed by Busso et al. (2001) and more recently by Travaglio et al. (2004). The yield of Zr via the main *s*-process depends strongly on the size of the ^{13}C pocket, as this isotope is the source of the neutrons for this channel. The ^{13}C is itself produced locally within the AGB star by proton captures on the abundant isotope ^{12}C, but the requirement of having substantial C together with protons in a region hot enough for these reactions to proceed leads to these reactions occurring under very constrained conditions, as described in detail in Busso et al. (2001). The weak *s*-process, also involved in Zr production, utilizes ^{22}Ne as the neutron source. Karakas & Lattanzio (2007) provides an estimate of the total yield of elements heavier than the Fe-peak (i.e., beyond the maximum atomic mass included in their reaction network) in AGB stars. Their results suggest that the production of Zr is biased towards lower mass AGB stars than those within which the heavy isotopes of Mg are made, which could explain why [Zr/Fe] does not appear to vary among the M71 giants in our sample. Better models to verify the consistency of our results with the predicted behavior of Zr and La versus the Mg isotope ratios in AGB stars as a function of mass are needed.

Eu serve the same role for the *r*-process of neutron capture which produces selected isotopes of heavy elements beyond the Fe peak. No credible star-to-star variations could be detected among the luminous M71 giants in [Eu/Fe] based on the strength of the 6645 Å line of Eu II.

5. CONCLUSIONS

With the aid of exquisite spectral resolution and very high signal-to-noise spectra combined with a very careful analysis, we have determined Mg isotopic ratios for 9 luminous giants in the metal-rich Galactic globular cluster M71. We have also used these spectra to determine precision abundances for several other elements in this GC, including the light elements O, Na, Mg, and Al.

The abundances of Si, Ca, Ti, Ni and Fe do not show any star-to-star variations. The total range for the absolute Fe abundance, log[ϵ(Fe)], among the sample of nine giants in M71 is only 0.08 dex. Once the dependence on $T_{\rm eff}$ is removed, all the M71 giants have identical [Fe/H], [Si/Fe], [Ca/Fe], [Ti/Fe], and [Ni/Fe] to within $\sigma = 0.04$ dex (10%). This places a strong constraint on the uniformity of mixing in the young GC. These elements cannot have been produced in anything other than the first generation of GC stars.

We see the expected correlations and anticorrelations among the light elements O, Na, Mg, and Al in the M71 giants. But the amplitude of the star-to-star variations among these elements is small, 0.3 dex for [O/Fe], 0.6 dex for [Na/Fe], 0.2 dex for [Al/Fe], and at most 0.1 dex for [Mg/Fe]. Carretta et al. (2007) have looked for a link between chemical anomalies along the RGB and other properties of GCs. In addition to the obvious suggestion that higher amplitude star-to-star variations should be found in higher mass GCs, which with their higher binding energies may be better able to retain stellar ejecta, they suggest that the high temperature extension of the horizontal branch blue tail is longer in GCs with higher amplitude Na-O anticorrelations. The latter is attributed to a spread in He, and hence may again be tied to the ability to retain ejected gas, see the discussion in Carretta et al. (2007). We suggest that one additional parameter is relevant, the Fe-metallicity of the GC. As the stellar metallicity becomes higher, the effect of the addition of AGB processed material, whose nucleosynthesis proceeds among the light elements in a manner which is somewhat independent of their initial metallicity, would be diluted, and the resulting yield, assumed to be positive, reduced. Such an effect is apparent in the calculation of AGB yields by Karakas & Lattanzio (2007), among others. This would explain why the most prominent cases of star-to-star variations within GCs are seen among the lower metallicity GCs (i.e. M15, M13, etc) even though there are a number of quite massive high-metallicity GCs such as 47 Tuc for which Carretta et al. (2004) found only modest star-to-star variations among the light elements. In this context it is interesting to note that the behavior of CH and CN bands in these relatively high metallicity GCs tends to be bimodal, while in more metal-poor GCs, stars fill the entire range of C and N abundances without being so concentrated towards the upper and lower extremes of [C/Fe] (see e.g., Figure 11 of Cohen et al. 2005).

The heavy Mg isotopes among the CN weak giants in our M71 sample have very low Mg isotopic ratios ^{26}Mg/Mg ($\sim$4%) which are consistent with models of galactic chemical evolution with no contribution from AGB stars. These stars are both CN weak and have light element abundances typical of field Galactic halo metal-poor stars of similar Fe-metallicity; we call them the "normal" stars. Kroupa & Boily (2002) discuss forming the Galactic halo field via dissolved GCs; our results suggest that this must have involved the "normal" GC stars from clusters which dissolved early on before their intermediate-mass stars reached the AGB. The CN strong M71 giants have higher Mg isotopic ratios ^{26}Mg/Mg ($\sim$8%), but these are far below previously published values by Yong et al. (2006) and references therein for more metal-poor GC giants. This group of stars, in addition to a higher fraction of the heavier Mg isotopes, shows enhanced Na and Al, accompanied by lower O abundances.

The behavior of the Mg isotopes in the "normal" stars is reproduced by models of galactic chemical evolution by Fenner et al. (2003) without any contribution from AGB stars. Their models with the AGB contribution expected in the normal course of stellar evolution reproduce the behavior of the heavy Mg isotope rich M71 giants. These stars must represent a later generation of stars formed sufficiently long after the first that the AGB contribution to their chemical inventory was included.

[7] The Ba II lines are too strong to be able to detect the small star-to-star variations seen here.

Alternatively, the CN-rich and CN-weak stars may have formed at the same time, but the CN-weak stars could have been formed in an unmixed environment, while the CN-strong stars were born from material polluted by AGB stars.

With the present work, we believe we have demonstrated convincingly that the difference between the generations of GC stars is consistent in detail with the contribution of AGB stars. Furthermore, we have extended our previous results from Meléndez & Cohen (2007) based on metal-poor halo field dwarfs to still higher metallicity, up to the Fe-metallicity of M71. Based on the calculations of stellar yields for AGB stars by Karakas & Lattanzio (2003), updated in Karakas & Lattanzio (2007), stars of initial mass 3–6 $M_{\odot}$ are required to contribute significant amounts of the heavier Mg isotopes. Stellar evolutionary tracks establish that stars in this mass range reach the upper AGB at an age of ∼0.3 Gyr. Assuming uniform mixing within the gas in this GC, for a GC as metal-rich as is M71, this timescale must reflect the minimum age difference between the CN-weak and the CN-rich stars in the GC and the maximum age range of the CN-weak stars we see today. Furthermore, the enrichment of the halo gas from which M71 eventually formed must have reached such a high Fe-metallicity without a substantial contribution of "polluted" material, whose source we argue on the basis of the tight constraints we have placed on any variation in abundance among the Fe-peak elements in M71 must be AGB stars.

The entire Keck/HIRES user community owes a huge debt to Jerry Nelson, Gerry Smith, Steve Vogt, and many other people who have worked to make the Keck Telescope and HIRES a reality and to operate and maintain the Keck Observatory. We are grateful to the W. M. Keck Foundation for the vision to fund the construction of the W. M. Keck Observatory. The authors wish to extend special thanks to those of Hawaiian ancestry on whose sacred mountain we are privileged to be guests. Without their generous hospitality, none of the observations presented herein would have been possible.

We are grateful to NSF grant AST-0507219 and FCT (project PTDC/CTE-AST/65971/2006 and Ciencia 2007) for partial support. We thank B. Plez for providing the CH line list, and D. Yong and W. Aoki for sharing their spectrum of M71 A4. This publication makes use of data from the 2MASS, which is a joint project of the University of Massachusetts and the Infrared Processing and Analysis Center, funded by the National Aeronautics and Space Administration and the National Science Foundation.

REFERENCES

Asplund, M. 2005, ARA&A, 43, 481
Briley, M. M., & Cohen, J. G. 2001, AJ, 122, 242
Busso, M., Gallino, R., Lambert, D. L., Travaglio, C., & Smith, V. V. 2001, ApJ, 557, 802
Carretta, E., Gratton, R. G., Bragaglia, A., Bonifacio, P., & Pasquini, L. 2004, A&A, 416, 925
Carretta, E., Recio-Blanco, A., Gratton, R. G., Piotto, G., & Bragaglia, A. 2007, ApJ, 671, L125
Castelli, F., Gratton, R. G., & Kurucz, R. L. 1997, A&A, 318, 841
Cohen, J. G., Behr, B. B., & Briley, M. M. 2001, AJ, 122, 1420
Cohen, J. G., Briley, M. M., & Stetson, P. B. 2005, AJ, 130, 1177
Cohen, J. G., & Meléndez, J. 2005, AJ, 129, 303
Collet, R., Asplund, M., & Trampedach, R. 2007, A&A, 469, 687
Cutri, R. M., et al. 2003, Explanatory Supplement to the 2MASS All-Sky Data Release, http://www.ipac.caltech.edu/2mass/releases/allsky/doc/explsup.html
da Silva, L., et al. 2006, A&A, 458, 609
Decressin, T., Meynet, G., Charbonnel, C., Prantzos, N., & Ekstrom, S. 2007, A&A, 464, 1029
Demarque, P., Woo, J.-H., Kim, Y.-C., & Yi, S. K. 2004, ApJS, 155, 667
Denisenkov, P. A., & Denisenkova, S. N. 1990, Sov. Astron. Lett., 16, 275
Fenner, Y., et al. 2003, Publ. Astron. Soc. Aust., 20, 340
Gay, P. L., & Lambert, D. L. 2000, ApJ, 533, 260
Gratton, R., Sneden, C., & Carretta, E. 2004, ARA&A, 42, 385
Gratton, R., et al. 2001, A&A, 369, 87
Harris, W. E. 1996, AJ, 112, 1487
Hekker, S., & Meléndez, J. 2007, A&A, 475, 1003
Hirschi, R., et al. 2008, 10th Symp. on Nuclei in the Cosmos, in press (arXiv:0811.4654)
Karakas, A. I., & Lattanzio, J. C. 2003, PASA, 20, 279
Karakas, A., & Lattanzio, J. C. 2007, PASA, 24, 103
Kroupa, P., & Boily, C. M. 2002, MNRAS, 336, 1188
Lawler, J. E., Bonvallet, G., & Sneden, C. 2001, ApJ, 556, 452
Lee, S.-G. 2005, J. Korean Astron. Soc., 38, 23
McWilliam, A., & Lambert, D. L. 1988, MNRAS, 230, 573
Meléndez, J., & Asplund, M. 2008, A&A, 490, 817
Meléndez, J., & Barbuy, B. 1999, ApJS, 124, 527
Meléndez, J., & Barbuy, B. 2009, A&A, 497, 611
Meléndez, J., & Cohen, J. G. 2007, ApJ, 659, L25
Meléndez, J., et al. 2008, A&A, 484, L21
Plez, B., & Cohen, J. G. 2005, A&A, 434, 1117
Plez, B., et al. 2008, in ASP Conf. Ser. 384, 14th Cambridge Workshop on Cool Stars, Stellar Systems, and the Sun, ed. G. van Belle (San Francisco, CA: ASP), 384 (poster)
Ramírez, I., & Meléndez, J. 2005, ApJ, 626, 465
Ramírez, S., & Cohen, J. G. 2002, AJ, 123, 3277
Shetrone, M. D. 1996, AJ, 112, 2639
Skrutskie, M. F., et al. 1997, in The Impact of Large Scale Near IR Sky Surveys, ed. F. Garzon et al. (Dordrecht: Kluwer), 187
Smith, G. H., & Norris, J. 1982, ApJ, 254, 149
Smith, V. V., Cunha, K., Ivans, I. I., Lattanzio, J. C., Campbell, S., & Hinkle, K. H. 2005, ApJ, 633, 392
Sneden, C. A. 1973, PhD thesis, Univ. of Texas at Austin
Stetson, P. B. 2000, PASP, 112, 925
Travaglio, C., Gallino, R., Arnone, E., Cowan, J. C., Jordan, F., & Sneden, C. 2004, ApJ, 601, 864
Ventura, P., & D'Antona, F. D. 2008, MNRAS, 385, 2034
Vogt, S. S., et al. 1994, Proc. SPIE, 2198, 362
Woosley, S. E., & Weaver, T. A. 1995, ApJ, 101, 181
Yong, D., Aoki, W., & Lambert, D. L. 2006, ApJ, 638, 1018
Yong, D., Grundahl, F., D'Antona, F., Karakas, A. I., Lattanzio, J. C., & Norris, J. E. 2009, ApJ, 695, L62
Yong, D., Grundahl, F., Lambert, D. L., Nissen, P. E., & Shetrone, M. D. 2003, A&A, 402, 985
Yong, D., Meléndez, J., Cunha, K., Karakas, A. I., Norris, J. E., & Smith, V. V. 2008, ApJ, 689, 1020